

it is linked to a bidentate chelating nitrate on one side of the macrocycle and to a second bidentate chelating nitrate and a methanol molecule on the other side. Thus, it becomes difficult to determine whether the greater degree of planarity of the Sr-L³ complex compared to the Pr-L⁴ analogue results from the lower metal coordination number, from the absence of the four sterically hindering methyl groups, or from a combination of both factors. The structures of only two other complexes of L³, those of the isomorphous pair [CdL³(H₂O)(ClO₄)](ClO₄)·CH₃OH and [PbL³(H₂O)](ClO₄)₂·H₂O, have been reported.³³ In the Cd complex the metal ion is 8-coordinate and has an approximate hexagonal-bipyramidal geometry, being bonded to a water molecule and a perchlorate oxygen atom in the axial positions. In the Pb complex, the two perchlorates are ionic and the water molecule is axially coordinated to the metal on one side of the macrocycle, leaving the opposite side completely free or, rather,

as the authors suggest, occupied by a stereochemically active Pb lone pair. The macrocycle is described as nearly planar, giving further support to the idea that the steric hindrance of the axially coordinated ligands has a determining influence on the macrocycle conformation.

Acknowledgment. We wish to thank Mr. James D. Spivey for the electron microscope examinations and Mr. Mark A. Benvenuto (Department of Chemistry, University of Virginia) for the measurement of mass spectra. We also acknowledge the financial support of a VCU Grant-In-Aid, of Coulter Electronics, Hialeah, FL, and of NATO Bilateral Project No. 184-85.

Supplementary Material Available: Tables IA, IIA, and IVA, listing crystal data, fractional hydrogen coordinates, and C, H, and N microanalyses (3 pages); Table IIIA, listing structure factors (18 pages). Ordering information is given on any current masthead page.

Contribution from the Department of Chemistry,
University of Hawaii, Honolulu, Hawaii 96822

Unusual Reversible Dimerization of a μ -Pyridine-2-thiolato (pyS) Complex: Crystal Structure of Pd₂(μ -N-S- η^2 -pyS)₂Cl₂(PMe₃)₂

John H. Yamamoto, Wesley Yoshida, and Craig M. Jensen*

Received June 1, 1990

Reaction of [PdCl(PMe₃)(μ -Cl)]₂ with sodium pyridine-2-thiolate in ethanol gives rise to Pd₂(μ -N-S- η^2 -pyS)₂Cl₂(PMe₃)₂ (**1**). Variable-temperature ¹H and ³¹P{¹H} NMR spectra of **1** indicate fluxional behavior associated with the bridging pyS ligands. The dramatic temperature-dependent shift in the equilibrium position of the interconverting species demonstrates that a large entropy change is associated with the dynamic process. From the ratios of the changing integrated intensities of the signals in the ³¹P{¹H} NMR spectra over the -30 to +70 °C temperature range, values of $\Delta H = 26 \pm 1$ kJ mol⁻¹, $\Delta S = 75 \pm 3$ J K⁻¹ mol⁻¹ and $\Delta G_{293} = 4$ kJ mol⁻¹, for the fluxional process, can be calculated while similar analysis of the signals for the PMe₃ protons in ¹H NMR spectra over the 20–80 °C range are indicative of similar energetic values of $\Delta H = 29 \pm 1$ kJ mol⁻¹, $\Delta S = 87 \pm 4$ J K⁻¹ mol⁻¹ and $\Delta G_{293} = 4$ kJ mol⁻¹. The signals for the trimethylphosphine protons are observed to coalesce at 97 °C, and this thus allows calculation of a ΔG^\ddagger of 72 kJ mol⁻¹ for the dynamic process. Variable-temperature ¹³C {¹H} NMR spectroscopy indicates that the dynamic process involves interconverting η^2 -pyS complexes. Molecular weight determinations by measurement of carbon tetrachloride boiling-point elevation demonstrate that a monopalladium complex is the predominant species present at elevated temperatures. The crystal and molecular structure of **1**·EtOH has been determined. Crystallographic data for **1**·EtOH: orthorhombic *Pbca*, *Z* = 8, *a* = 12.588 (4) Å, *b* = 20.08 (1) Å, *c* = 20.45 (1) Å, *V* = 5170 (5) Å³, $\rho_{\text{calcd}} = 1.737$ g/cm³.

Introduction

Complexes containing pyridine-2-thiolate, pyS, ligands in a variety of bridging coordination modes have recently been reported.^{1–3} Fluxional behavior involving bridging pyS ligands has been noted^{2,3a} for several of these complexes. Mechanisms involving eight-membered ring inversion as well as cleavage of a Pd–N bond followed by rotation about a Pd–S bond were considered by Deeming² for the exchange of diastereotopic methyl groups in Pd₂[2-(dimethylamino)phenyl]₂(μ -N-S- η^2 -pyS)₂, with the latter mechanism considered to be more likely. Alternatively, Oro^{3a} has proposed a mechanism involving intermediate μ -S-

η^2 -coordinated pyS ligands for intermolecular exchange of carbonyl groups in Rh₂(pyS)₂(CO)₂ and proton exchange processes in Rh₂(pyS)₂(olefin)₂ complexes.

We have isolated Pd₂(μ -N-S- η^2 -pyS)₂Cl₂(PMe₃)₂ (**1**) and determined its molecular structure through a single-crystal X-ray diffraction study. In solution, **1** is seen by ¹H, ¹³C, and ³¹P NMR spectroscopy to establish a highly temperature-dependent equilibrium with a second species. Our variable-temperature NMR studies and molecular weight determinations indicate that a rapid equilibrium is established between the dimetallic complex, **1**, and a monometallic Pd(pyS)Cl(PMe₃) complex. The (μ -halo)di-palladium complexes, Pd₂(μ -X)₂X₂(PR₃)₂ (X = Cl, Br) have long been believed⁴ to undergo rapid dimer–monomer interconversion in solution. However, monomeric intermediates have not been considered in the fluxional behavior of dimetallic μ - η^2 -pyS complexes due to the high thermal stability that has generally been found⁵ for monomeric pyS complexes. We herein report the synthesis and molecular structure of **1** along with the results of our studies of this complex by variable-temperature ¹H, ³¹P, and ¹³C NMR spectroscopy.

- (1) (a) Kinoshita, I.; Yasuba, Y.; Matsumoto, K.; Ooi, S. *Inorg. Chim. Acta* **1983**, *80*, L13–L14. (b) Deeming, A. J.; Meah, M. N.; Dawes, H. M.; Hursthouse, M. B. *J. Organomet. Chem.* **1986**, *299*, C25–C28. (c) Umakoshi, K.; Kinoshita, I.; Ooi, S. *Inorg. Chim. Acta* **1987**, *80*, L41–L42. (d) Deeming, A. J.; Meah, M. N.; Bates, P. A.; Hursthouse, M. B. *J. Chem. Soc., Dalton Trans.* **1988**, 235–238. (e) Deeming, A. J.; Karim, M.; Bates, P. A.; Hursthouse, M. B. *Polyhedron* **1988**, *7*, 1401–1403. (f) Padilla, E. M.; Yamamoto, J. H.; Jensen, C. M. *Inorg. Chim. Acta* **1990**, *174*, 209–215.
- (2) Deeming, A. J.; Meah, M. N.; Bates, P. A.; Hursthouse, M. B. *J. Chem. Soc., Dalton Trans.* **1988**, 2193–2199.
- (3) (a) Ciriano, M. A.; Viguri, F.; Torrente-Perez, J. J.; Lahoz, F. J.; Oro, L. A.; Tiripicchio, A.; Tiripicchio-Camellini, M. *J. Chem. Soc., Dalton Trans.* **1990**, 25–32. (b) Ciriano, M. A.; Torrente-Perez, J. J.; Viguri, F.; Lahoz, F. J.; Oro, L. A.; Tiripicchio, A.; Tiripicchio-Camellini, M. *J. Chem. Soc., Dalton Trans.* **1990**, 1493–1502.

- (4) (a) Chatt, J.; Venanzi, L. M. *J. Chem. Soc.* **1957**, 2445. (b) Cotton, F. A.; Wilkinson, G. *Advanced Inorganic Chemistry*, 4th ed.; John Wiley: New York, 1980; p 952.
- (5) Deeming, A. J.; Meah, M. N.; Randle, N. P.; Hardcastle, K. I. *J. Chem. Soc., Dalton Trans.* **1989**, 2211–2216.

Table I. Summary of Crystal Data for $\text{Pd}_2\text{Cl}_2(\mu\text{-pyS})_2(\text{PMe}_3)_2\cdot\text{EtOH}$

formula	$\text{Pd}_2\text{Cl}_2\text{P}_2\text{S}_2\text{C}_{18}\text{N}_2\text{OH}_{32}$
fw	651.6
cryst dims, mm	$0.1 \times 0.1 \times 0.1$
cryst syst	orthorhombic
space group	<i>Pbca</i>
<i>a</i> , Å	12.588 (4)
<i>b</i> , Å	20.08 (1)
<i>c</i> , Å	20.45 (1)
<i>V</i> , Å ³	5170 (5)
<i>Z</i>	8
ρ_{calc} , g/cm ³	1.737
λ , Å (Mo K α radiation)	0.710 73
<i>T</i> , K	297
scan type	ω
scan rate, deg/min	1.5–15
2 θ range, deg	4.0–45.0
μ , cm ⁻¹	18.70
transm coeff	0.558–0.614
no. of reflections collcd	2866
no. of unique data with $I > 3\sigma(I)$	1733
R , %	2.54
R_w , %	2.21
goodness of fit ^c	1.37

$$^a R = \frac{\sum |F_o| - |F_c|}{\sum F_o} \quad ^b R_w = \frac{[\sum w(|F_o| - |F_c|)^2 / \sum w F_o^2]}{1/2}$$

$$^c \text{GOF} = \frac{[\sum w(|F_o| - |F_c|)^2 / (N_o - N_v)]^{1/2}}$$

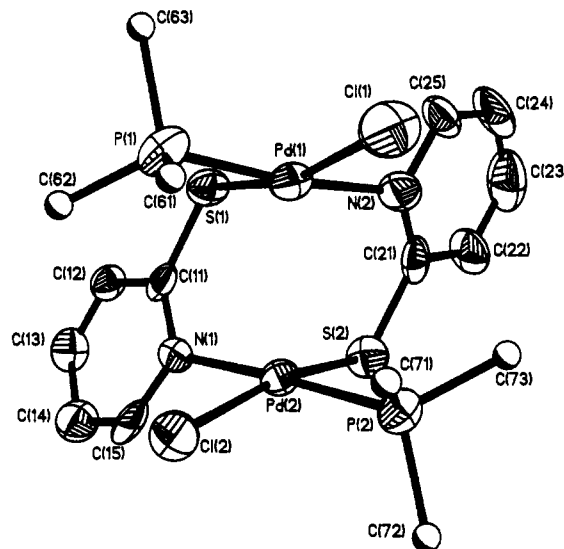
Experimental Section

General Details. The following were purchased from Aldrich Chemical Co. and used without further purification: 2-thiopyridine, dichloromethane (reagent grade), chloroform-*d*₁, toluene-*d*₈, and dichloromethane-*d*₂. Ethanol (absolute) was purchased from Quantum Chemical Corp. The complex $[\text{PdCl}(\text{PMe}_3)(\mu\text{-Cl})_2]$ was prepared by a method analogous to the Chatt and Venanzi⁶ synthesis of $[\text{PdCl}(\text{PEt}_3)(\mu\text{-Cl})_2]$.

The ¹³C{¹H} and ³¹P{¹H} NMR spectra were recorded on a GN Omega 500 spectrometer at 125.8 and 202.4 MHz, respectively. The ¹H NMR spectra were recorded on a Nicolet NT300 spectrometer at 300 MHz. The ¹H NMR data are listed in ppm downfield from TMS at 0.00 ppm. ³¹P NMR chemical shifts were measured relative to the deuterium resonance of the solvent by using the internal frequency lock of the spectrometer so that the resonance from a capillary of 85% H₃PO₄, centered in a 5 mm NMR tube containing the deuterated solvent, appeared at 0.0 ppm at 20 °C. A preacquisition delay of 100 μs and a pulse delay of 3 s were used in the variable-temperature ¹H NMR studies while a preacquisition delay of 56 μs and a pulse delay of 3 s were used in the variable-temperature ³¹P NMR experiments.

Preparation of $\text{Pd}(\mu\text{-N-S-}\eta^2\text{-pyS})_2\text{Cl}_2(\text{PMe}_3)_2$ (1). An ethanolic solution of sodium ethoxide under nitrogen (prepared by dissolving 0.025 g (1.105 mmol) of sodium in 40 mL of absolute ethanol) is treated with pyridine-2-thiol (0.110 g, 0.989 mmol). Under nitrogen purge, $[\text{PdCl}(\text{PMe}_3)(\mu\text{-Cl})_2]$ (0.250 g, 0.494 mmol) is added to the clear, yellow solution arising upon completion of the heterocycle deprotonation, and the resulting suspension is allowed to stir for 24 h. The resulting air-stable orange solid is isolated by filtration from the reaction mixture. The product is extracted with 10 mL of dichloromethane and the residual NaCl is separated by filtration. The microcrystalline, orange product is isolated upon removal of the dichloromethane under vacuum (0.248 g, 76.5% yield). ¹H NMR (toluene-*d*₈, -40 °C): δ 8.71 (1 H, br s), 7.15 (1 H, m), 6.32 (1 H, m), 6.07 (1 H, m) (aromatic); 1.43 (18 H, d, $J_{\text{P-H}} = 12$ Hz) ($\text{P}(\text{CH}_3)_3$). ¹³C{¹H} NMR (toluene-*d*₈, -30 °C): δ 168.4 (s) (S-C); 151.4 (s), 134.5 (s), 127.4 (s) 118.0 (s) (aromatic); 14.9 (d, $J_{\text{P-C}} = 36.6$ Hz) ($\text{P}(\text{CH}_3)_3$). ³¹P{¹H} NMR (toluene-*d*₈, -50 °C): δ 6.1 (s). Anal. (Onedia Research Services Inc., Whitesboro, NY) Calcd: C, 29.29; H, 3.99; N, 4.27. Found: C, 29.95; H, 4.17; N, 4.02.

Molecular Weight Determinations. Molecular weight determinations were carried out by a literature^{7a} method utilizing a Lauda RC6 temperature controller and a Beckmann thermometer. The temperature difference between the boiling point of a 0.783-g sample of pure CCl₄ and equal amounts of CCl₄ into which 0.004 g of 1 had been dissolved was observed to be consistently 0.08 ± 0.01 °C. On the basis of a value

**Figure 1.** ORTEP projection of $\text{Pd}_2(\mu\text{-N-S-}\eta^2\text{-pyS})_2\text{Cl}_2(\text{PMe}_3)_2$ (1); thermal ellipsoids at 50% probability. The hydrogen atoms have been omitted, and the PMe_3 carbons are shown at an arbitrary radius for clarity.**Table II.** Selected Bond Distances (Å) and Angles (deg) for $\text{Pd}_2\text{Cl}_2(\mu\text{-pyS})_2(\text{PMe}_3)_2\cdot\text{EtOH}$

Distances			
Pd(1)–S(1)	2.284 (3)	Pd(2)–S(2)	2.306 (3)
Pd(1)–N(2)	2.137 (9)	Pd(2)–N(1)	2.131 (8)
Pd(1)–P(1)	2.243 (4)	Pd(2)–P(2)	2.244 (3)
Pd(1)–Cl(1)	2.356 (3)	Pd(2)–Cl(2)	2.355 (3)
S(1)–C(11)	1.73 (1)	S(2)–C(21)	1.73 (1)
Angles			
S(1)–Pd(1)–N(2)	88.3 (2)	S(2)–Pd(2)–N(1)	88.0 (2)
N(2)–Pd(1)–Cl(1)	90.1 (3)	N(1)–Pd(2)–Cl(2)	90.0 (2)
Cl(1)–Pd(1)–P(1)	90.4 (1)	Cl(2)–Pd(2)–P(2)	89.7 (1)
S(1)–Pd(1)–P(1)	89.3 (1)	S(2)–Pd(2)–P(2)	91.6 (1)
P(1)–Pd(1)–N(2)	172.8 (3)	P(2)–Pd(2)–N(1)	176.9 (2)
S(1)–Pd(1)–Cl(1)	164.3 (1)	S(2)–Pd(2)–Cl(2)	167.2 (1)
Pd(1)–S(1)–C(11)	114.7 (4)	C(11)–N(1)–C(15)	116.9 (8)
Pd(2)–S(2)–C(21)	113.9 (4)	C(21)–N(2)–C(25)	119.8 (9)

of 4.48 as the ebullioscopic constant of carbon tetrachloride,^{7b} a molecular weight of 303 ± 43 was calculated^{7b} for the species present in solution at the boiling point (77 °C) of CCl₄.

Crystallographic Studies. Crystals suitable for X-ray diffraction were obtained by slow evaporation of a dichloromethane solution 1. The crystal was mounted on a glass fiber with epoxy and centered on a Nicolet P3 automated diffractometer. The unit cell parameters were obtained by least-squares refinement of the setting angles of 20 reflections. Crystal and instrument stability were monitored with a set of three standard reflections measured every 97 reflections; in all cases, no significant variations were found. Details of other crystal data and relevant information are summarized in Table I.

The structure was solved by direct methods using SHELX PLUS computer programs (Nicolet Instrument Corp.) and refined by full-matrix least-squares procedures. During the refinement, a group of peaks, not associated with the palladium complex became apparent in the difference Fourier maps. The peaks were refined isotropically as an ethanol solvate that is 2-fold disordered about an inversion center at the origin. All non-hydrogen atoms except those of the solvate were refined with anisotropic temperature coefficients. The hydrogen atoms were introduced in fixed calculated positions, and their coordinates were allowed to vary in the final cycles of full-matrix least-squares refinement.

Results and Discussion

Reaction of $[\text{PdCl}(\text{PMe}_3)(\mu\text{-Cl})_2]$ with 2 equiv of sodium pyridine-2-thiolate in ethanol solution gives $\text{Pd}_2(\mu\text{-N-S-}\eta^2\text{-pyS})_2\text{Cl}_2(\text{PMe}_3)_2$ (1) in 76% yield. The molecular structure of 1 was determined by a single-crystal X-ray structural diffraction study. An ORTEP projection with the atomic numbering scheme of the obtained molecular structure is seen in Figure 1. Bond angles and distances are listed in Table II; the final fractional

(6) Chatt, J.; Venanzi, L. M. *J. Chem. Soc.* **1957**, 2351–2356.

(7) (a) Pavia D. L.; Lampman, G. M.; Kriz G. S. *Introduction to Organic Laboratory Techniques*, 3rd ed.; Saunders: Philadelphia, PA, 1988; pp 552–554. (b) Dean, J. A. *Lange's Handbook of Chemistry*, 13th ed.; McGraw-Hill: New York, 1985; p (10)73.

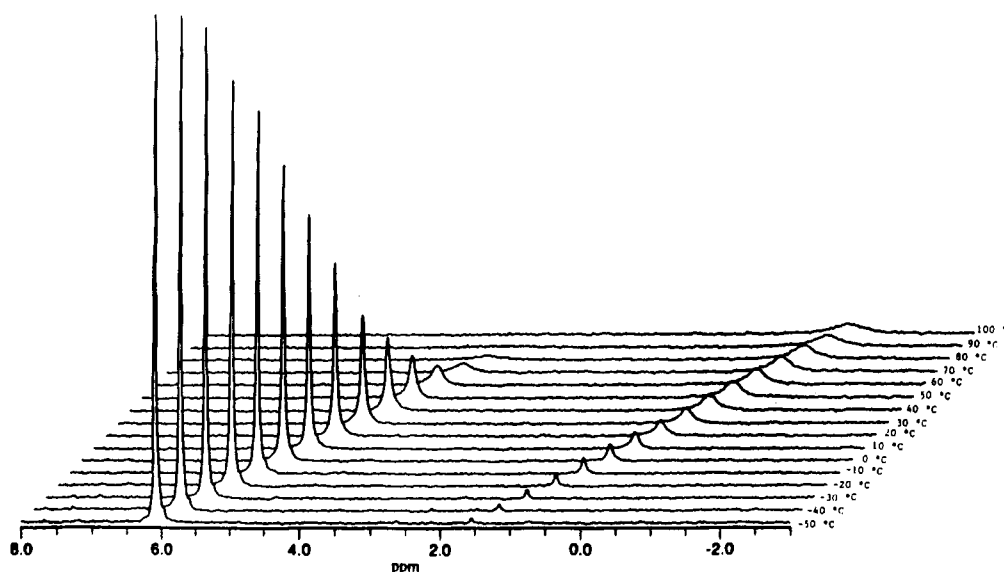


Figure 2. Variable-temperature $^{31}\text{P}\{^1\text{H}\}$ NMR (202.4 MHz) spectra of $\text{Pd}_2(\text{pyS})_2\text{Cl}_2(\text{PMe}_3)_2$ dissolved in toluene- d_8 .

atomic coordinates are given in Table III. The molecular structure has an approximately C_2 symmetry with the two palladium atoms linked through the two μ -pyS ligands in a head-to-tail fashion. The coordination geometry about each of the palladium atoms is nearly square planar. The chlorine atoms are oriented trans to the sulfur of the bridging ligand while the phosphines are oriented trans to the nitrogen of the bridging ligand. The Pd(1)–Pd(2) distance of 2.942 (2) Å clearly demonstrates the lack of Pd–Pd bonding. The angles C(11)–N(1)–C(15) and C(21)–N(2)–C(25) of 116.9 (8) and 119.8 (9)°, respectively, are within the range expected⁸ for deprotonated N-heterocycles. The C(11)–S(1) and C(21)–S(2) distances of 1.73 (1) and 1.73 (1) Å, respectively, are within the 1.72–1.86-Å range that has been found^{1–3,5,9} in pyS complexes and indicate that the bridging pyS ligands have a significant amount of thione character.

Variable-temperature $^{31}\text{P}\{^1\text{H}\}$ NMR spectra of **1** in toluene- d_8 are shown in Figure 2.¹⁰ A sharp resonance at 6.1 ppm and a much smaller one at 1.6 ppm are observed at -40 °C. The signals are seen to gradually broaden as the temperature is raised. Additionally, there is a continuous increase in the relative integrated intensity of the upfield resonance compared to that of the downfield resonance, reflecting a shift in the equilibrium position with temperature. Thus while the ratio of the downfield and upfield resonances is greater than 30:1 at -30 °C, it is less than 1:1.25 at 70 °C. When the solution is cooled, the trend is reversed and spectra identical with those initially obtained are produced with no loss of integrated intensity with equal number of acquisitions. From the changing ratios of the integrated intensities

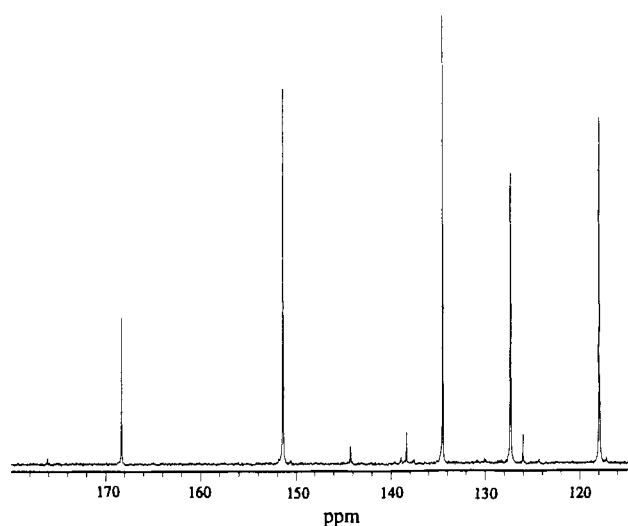


Figure 3. Aromatic region of the $^{13}\text{C}\{^1\text{H}\}$ NMR (125.8 MHz) spectrum of $\text{Pd}_2(\text{pyS})_2\text{Cl}_2(\text{PMe}_3)_2$ dissolved in chloroform- d at -40 °C.

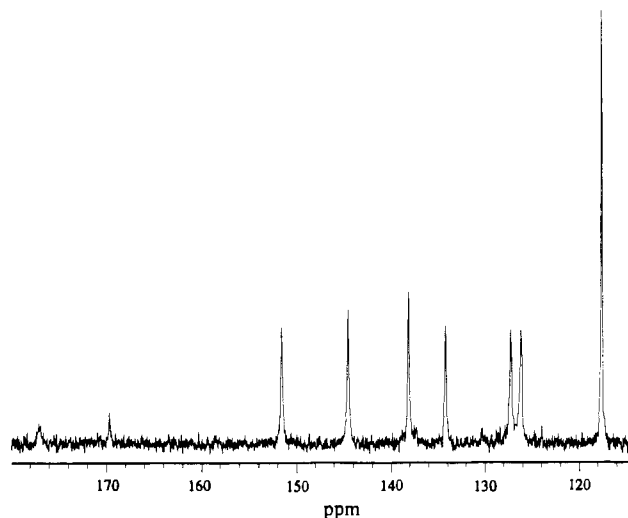


Figure 4. Aromatic region of the $^{13}\text{C}\{^1\text{H}\}$ NMR (125.8 MHz) spectrum of $\text{Pd}_2(\text{pyS})_2\text{Cl}_2(\text{PMe}_3)_2$ dissolved in chloroform- d at 50 °C.

of the two signals over the -30 to $+70$ °C temperature range, values of $\Delta H = 26 \pm 1$ kJ mol⁻¹, $\Delta S = 75 \pm 3$ J K⁻¹ mol⁻¹ and $\Delta G_{293} = 4$ kJ mol⁻¹, for the fluxional process, can be calculated.

(8) Singh, C. *Acta Crystallogr.* **1965**, *19*, 861–864.

(9) (a) Fletcher, S. R.; Skapski, A. C. *J. Chem. Soc., Dalton Trans.* **1972**, 635–639. (b) Cotton, F. A.; Fanwick, P. E.; Fitch, J. W. *Inorg. Chem.* **1978**, *17*, 3254–3257. (c) Masaki, M.; Matsunami, S.; Ueda, H. *Bull. Chem. Soc. Jpn.* **1978**, *51*, 3298–3301. (d) Mura, P.; Olby, B. G.; Robinson, S. D. *J. Chem. Soc., Dalton Trans.* **1985**, 2101–2112. (e) Rosenfield, S. G.; Swedberg, S. A.; Arora, S. K.; Mascharak, P. K. *Inorg. Chem.* **1986**, *25*, 2109–2114. (f) Rosenfield, S. G.; Berends, H. P.; Gelmini, L.; Stephan, D. W.; Mascharak, P. K. *Inorg. Chem.* **1987**, *26*, 2792–2797. (g) Deeming, A. J.; Hardcastle, K. I.; Meah, M. N.; Bates, P. A.; Dawes, H. M.; Hursthouse, M. B. *J. Chem. Soc., Dalton Trans.* **1988**, 227–233.

(10) The total integrated area of the signals in variable-temperature ^{31}P NMR spectra appears to diminish with increasing temperature as the resonances approach coalescence and broaden. This effect is the result of signal lost into the baseline and not the result of “disappearing” phosphorus. Due to the highly temperature dependent solubility of **1**, very dilute (0.003 g/1.5 mL) samples had to be used in the variable-temperature experiments. It was not feasible in the ^{31}P NMR experiments to obtain the necessary signal to noise level to achieve fully consistent integrations as the resonances became significantly broadened. This effect is not seen for signals of the PMe_3 methyl protons in the variable-temperature ^1H NMR studies in which improved signal to noise can be achieved.

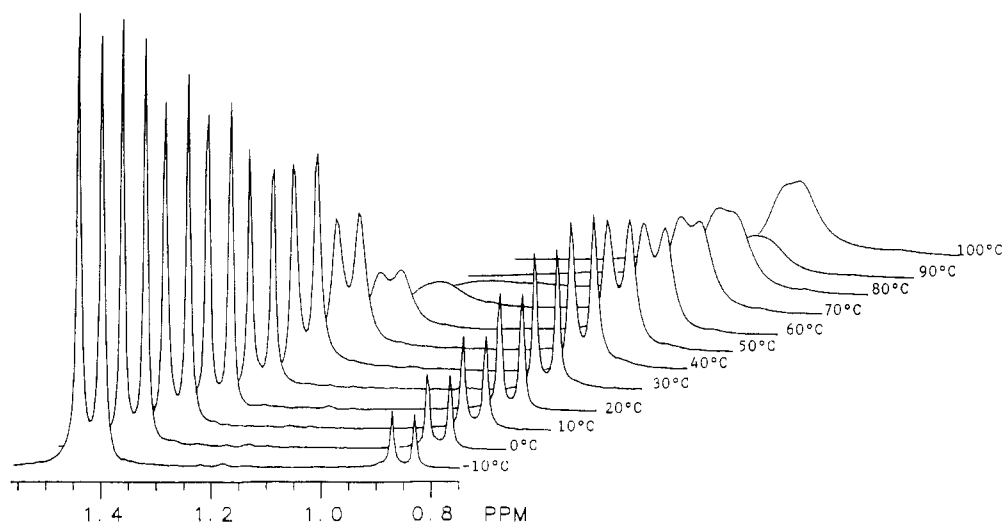


Figure 5. Variable-temperature ^1H NMR spectra (300 MHz) of the PMe_3 protons of $\text{Pd}_2(\text{pyS})_2\text{Cl}_2(\text{PMe}_3)_2$ dissolved in toluene- d_8 .

Table III. Atomic Coordinates and Equivalent Isotropic Displacement Coefficients^a for $\text{Pd}_2\text{Cl}_2(\mu\text{-pyS})_2(\text{PMe}_3)_2\cdot\text{EtOH}$

	<i>x</i>	<i>y</i>	<i>z</i>	$U_{\text{eq}}, \text{\AA}^2$
Pd(1)	-0.1964 (1)	0.6184 (1)	0.1468 (1)	0.038 (1)
Pd(2)	0.0216 (1)	0.6655 (1)	0.1702 (1)	0.032 (1)
Cl(1)	-0.2028 (3)	0.5501 (2)	0.0531 (1)	0.073 (1)
Cl(2)	0.0559 (2)	0.7520 (2)	0.0957 (1)	0.050 (1)
S(1)	-0.2371 (2)	0.6750 (1)	0.2405 (1)	0.041 (1)
S(2)	0.0226 (2)	0.5887 (1)	0.2541 (1)	0.043 (1)
P(1)	-0.2555 (3)	0.7052 (2)	0.0882 (1)	0.048 (1)
P(2)	0.0993 (2)	0.5928 (2)	0.1018 (1)	0.040 (1)
N(1)	-0.0440 (7)	0.7356 (4)	0.2374 (4)	0.031 (3)
N(2)	-0.1604 (7)	0.5335 (4)	0.2058 (4)	0.044 (4)
C(11)	-0.1410 (8)	0.7306 (5)	0.2660 (5)	0.035 (4)
C(12)	-0.1683 (9)	0.7736 (5)	0.3200 (5)	0.036 (4)
C(13)	-0.099 (1)	0.8196 (6)	0.3410 (5)	0.041 (5)
C(14)	-0.003 (1)	0.8276 (6)	0.3081 (6)	0.049 (6)
C(15)	0.0199 (9)	0.7849 (6)	0.2587 (6)	0.041 (5)
C(21)	-0.0786 (9)	0.5307 (5)	0.2493 (6)	0.040 (4)
C(22)	-0.076 (1)	0.4785 (6)	0.2960 (6)	0.053 (5)
C(23)	-0.152 (1)	0.4311 (7)	0.2962 (8)	0.075 (7)
C(24)	-0.234 (1)	0.4342 (6)	0.2500 (9)	0.071 (7)
C(25)	-0.2361 (9)	0.4851 (7)	0.2059 (7)	0.053 (5)
C(61)	-0.204 (1)	0.7087 (9)	0.0055 (7)	0.076 (7)
C(62)	-0.235 (1)	0.7882 (8)	0.1172 (7)	0.069 (6)
C(63)	-0.398 (1)	0.697 (1)	0.0797 (6)	0.069 (7)
C(71)	0.065 (1)	0.6055 (7)	0.0164 (6)	0.056 (5)
C(72)	0.244 (1)	0.6000 (8)	0.1026 (6)	0.068 (6)
C(73)	0.075 (1)	0.5049 (8)	0.1132 (8)	0.065 (7)
O(1)	-0.490 (3)	-0.501 (3)	-0.025 (2)	0.21 (2)
C(1)	0.506 (4)	0.445 (2)	0.023 (3)	0.18 (2)
C(2)	0.590 (3)	0.456 (2)	0.057 (2)	0.15 (2)

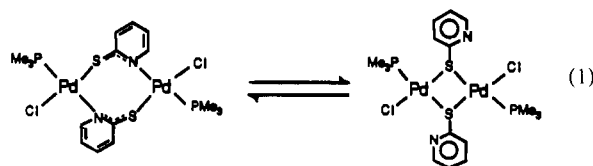
^a Equivalent isotropic U defined as one-third of the trace of the orthogonalized U_{ij} tensor.

This shift in equilibrium can also be observed by ^{13}C NMR spectroscopy. The aromatic region of the $^{13}\text{C}\{^1\text{H}\}$ NMR spectrum of a solution of **1** dissolved in chloroform- d at -40°C is seen in Figure 3. When the sample is warmed to 50°C , the aromatic region appears as seen in Figure 4. At this temperature a second set of aromatic carbon resonances are seen at 177.1, 151.8, 144.5, and 138.1 ppm while the resonance at 117.6 ppm now has approximately double intensity due to accidental overlap with one of the resonances of the species that was predominant at low temperature. Additionally, a second doublet ($J_{\text{P-C}} = 37$ Hz) due to the PMe_3 carbons of the new species is seen to arise at 14.9 ppm.

The appearance of the signals for the trimethylphosphine protons in the ^1H NMR spectrum of **1** in toluene- d_8 show a similar temperature dependence as seen in Figure 5. At -10°C sharp doublets at 1.42 ($J_{\text{P-H}} = 12$ Hz) and 0.83 ($J_{\text{P-H}} = 12$ Hz) ppm are observed. As the temperature is raised to 95°C , the signals are seen to broaden and the intensity of the upfield doublet in-

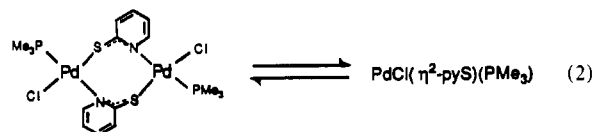
creases while that of the downfield doublet decreases. When the solution is cooled, the trend is reversed and spectra identical with those initially obtained are produced with no loss of integrated intensity with an equal number of acquisitions. The values of $\Delta H = 29 \pm 1$ kJ mol $^{-1}$, $\Delta S = 87 \pm 4$ J K $^{-1}$ mol $^{-1}$ and $\Delta G_{293} = 4$ kJ mol $^{-1}$, which are calculated from the changing ratios of the integrated intensities of the doublets over the -10 to $+70^\circ\text{C}$ temperature range, are in close agreement with those calculated from the variable-temperature $^31\text{P}\{^1\text{H}\}$ data. The signals for the trimethylphosphine protons are observed to coalesce at 97°C and this thus allows calculation of $\Delta G^\ddagger = 72$ kJ/mol for the dynamic process.

Fluxionality of complexes containing sulfur ligands is often associated with pyramidal inversion about coordinated sulfur.¹¹ However, the dramatic temperature-dependent shift in equilibrium position that we observe is inconsistent with a dynamic process involving interconversion of two conformers as equal populations of the conformers should be present at elevated temperatures. The equilibrium shift can be accounted for only a process involving a large entropy change. A process involving the rupture of Pd-N bonds and the establishment of $\mu\text{-S}$ -thiolato groups has been proposed by Oro^{3a} to account for scrambling of carbonyl groups in $\text{Rh}_2(\mu\text{-pyS})_2(\text{CO})_2$. Such a process would occur in our system as seen in eq 1. If such a process were occurring, the double-bond



character of the carbon-sulfur bond would be expected to greatly diminish. The α -carbon of the resulting thiolate group would therefore be expected to resonate significantly upfield from the 168 ppm chemical shift observed for the thione carbon of **1**. However, a new resonance appears *downfield* at 178 ppm in the $^{13}\text{C}\{^1\text{H}\}$ NMR spectrum at 50°C . This result is inconsistent with the formation of thiolate groups and indicates that the equilibrating species both contain groups of significant thione character.

A process whereby **1** simply undergoes dissociation to two $\text{PdCl}(\eta^2\text{-pyS})(\text{PMe}_3)$ monomers as seen in eq 2 is consistent with



both the large positive value of ΔS determined for the dynamic process as well as the ^{13}C NMR results. However, this possibility seemed unlikely due to the high thermal stability that has been observed⁵ for monometallic complexes containing pyS ligands. In order to establish whether the predominant species at elevated temperatures is a di- or monometallic species, we performed molecular weight determinations by measuring the elevation of the boiling point of carbon tetrachloride into which **1** was dissolved. The molecular weight of 303 ± 43 determined by these studies demonstrates that the species dominating the equilibrium at elevated temperatures is a monopalladium complex. Thus it appears that the observed dynamic process is rapid equilibrium between **1** and a monomeric $\text{PdCl}(\text{pyS})(\text{PMe}_3)$ complex.

Conclusion

Our studies indicate that in solution the dipalladium pyS complex **1** is in rapid equilibrium with a monomeric $\text{PdCl}(\eta^2\text{-pyS})(\text{PMe}_3)$ complex, clearly establishing that such species can rapidly interconvert at ambient conditions. Therefore, the interconversion of di- and monometallic $\eta^2\text{-pyS}$ complexes should be considered along with the mechanisms proposed previously by Deeming² and Oro³ for the fluxional behavior of dimetallic $\mu\text{-}\eta^2\text{-pyS}$ complexes.

We thank the University of Hawaii Research Council for the support of this research. The assistance of Mr. M. Mediati and Prof. R. E. Cramer in the X-ray diffraction study as well as helpful discussions with Prof. T. T. Bopp and Dr. Walter Niemczura is gratefully acknowledged.

Acknowledgment. We thank the University of Hawaii Research Council for the support of this research. The assistance of Mr. M. Mediati and Prof. R. E. Cramer in the X-ray diffraction study as well as helpful discussions with Prof. T. T. Bopp and Dr. Walter Niemczura is gratefully acknowledged.

Supplementary Material Available: Tables and plots of variable-temperature NMR data, a table of calculations of energetics, and tables of anisotropic thermal parameters, bond distances, bond angles, and hydrogen atom coordinates and isotropic thermal parameters for $\text{Pd}_2(\mu\text{-}N\text{-}S\text{-}\eta^2\text{-pyS})_2\text{Cl}_2(\text{PMe}_3)_2\cdot\text{EtOH}$ (7 pages); a table of structure factors (5 pages). Ordering information is given on any current masthead page.

Contribution from the Department of Chemistry, University of Louisville, Louisville, Kentucky 40292, School of Chemical Sciences, University of Illinois, Urbana, Illinois 61801, Department of Chemistry, University of California at San Diego, La Jolla, California 92093-0506, and Laboratoire de Chimie, Departement de Recherche Fondamentale Centre d'Etudes Nucléaires de Grenoble, 30841 Grenoble Cedex, France

Synthesis and Characterization of Dinuclear Copper(II) Complexes of the Dinucleating Ligand 2,6-Bis[bis((1-methylimidazol-2-yl)methyl)amino)methyl]-4-methylphenol

Kenneth J. Oberhausen,[†] John F. Richardson,[†] Robert M. Buchanan,^{*†} James K. McCusker,^{‡§} David N. Hendrickson,[§] and Jean-Marc Latour^{||}

Received December 14, 1989

The synthesis, crystal structures, and magnetic and spectroscopic properties are reported for a series of dinuclear copper(II) complexes of the novel dinucleating polyimidazole ligand 2,6-bis[bis((1-methylimidazol-2-yl)methyl)amino)methyl]-4-methylphenol (Hbimp). The copper complexes have both "open" ($[\text{Cu}_2(\text{bimp})(\text{H}_2\text{O})_2](\text{ClO}_4)_3$ (**2**) and $[\text{Cu}_2(\text{bimp})(\text{CH}_3\text{OH})_2](\text{ClO}_4)_3$ (**3**)) and "closed" ($[\text{Cu}_2(\text{bimp})(\text{OCH}_3)](\text{ClO}_4)_2$ (**4**) and $[\text{Cu}_2(\text{bimp})(\text{N}_3)](\text{ClO}_4)_2$ (**5**)) type structures. X-ray crystal structures of complexes **3** and **4** were determined with Mo $K\alpha$ radiation. Crystal data: **3**, $\text{C}_{31}\text{H}_{45}\text{N}_{10}\text{Cu}_2\text{Cl}_3\text{O}_{15}$, monoclinic, $P2_1/n$, $a = 17.855$ (3) Å, $b = 13.377$ (3) Å, $c = 18.054$ (4) Å, $\beta = 105.78$ (2)°, $Z = 4$, $R(F) = 0.051$ for 5074 independent data [$I \geq 3\sigma(I)$]; **4**, $\text{C}_{32}\text{H}_{48}\text{N}_{10}\text{Cu}_2\text{Cl}_2\text{O}_{12}$, monoclinic, $C2/c$, $a = 23.221$ (3) Å, $b = 12.903$ (2) Å, $c = 17.681$ (3) Å, $\beta = 125.34$ (1)°, $Z = 4$, $R(F) = 0.054$ for 2439 independent data [$I \geq 3\sigma(I)$]. In complex **3**, the copper ions are pentacoordinate, bonded to two imidazoles, a tertiary amine nitrogen, a methanol oxygen atom, and the bridging phenolate oxygen atom. The dinuclear complex has a $\text{Cu}(1)\text{-O}(1)\text{-Cu}(2)$ angle of 142.9 (2)° and a Cu-Cu separation of 4.090 (1) Å. In complex **4**, the copper ions also are pentacoordinate, bridged both by the phenolate oxygen atom and by a methoxide ion. The Cu-Cu' separation is 3.026 (1) Å with a $\text{Cu-O}(1)\text{-Cu'}$ angle of 98.7 (1)°. Magnetic susceptibility measurements reveal that there is no appreciable exchange interaction between the copper ions in complexes **2** and **5** ($|J| \leq 0.3 \text{ cm}^{-1}$), over the temperature range 2–300 K. In complex **4**, magnetic data indicate that the copper ions are involved in a moderate antiferromagnetic exchange interaction ($J = -47 \text{ cm}^{-1}$) over the temperature range 5–300 K. Differences in the strength of the magnetic exchange interactions are rationalized by using a magnetic orbital approach. UV-visible electronic spectral and EPR spectral data are presented for each complex.

Introduction

The synthesis of binuclear complexes containing histidyl imidazole functionalities as analogues of the ligating sites of complex metalloproteins is of current interest. This "synthetic analogue approach"¹ has been applied to modeling the active sites of the type III copper proteins hemocyanin (Hc) and tyrosinase (Ty).² Hemocyanin functions as an oxygen-transport protein in the hemolymph of several species of arthropods and mollusks, while tyrosinase is a monooxygenase enzyme. X-ray crystallographic data on deoxy-Hc indicate that the two $\text{Cu}(I)$ ions are separated by 3.8 ± 0.4 Å, with each copper bonded to two histidine residues at 2.0 Å and a third at 2.7 Å.³ Results from EXAFS⁴ and other spectroscopic studies^{2,5,6} indicate that when oxygen binds to deoxy-Hc, the histidine ligands remain coordinated and the Cu-Cu

separation is reduced to approximately 3.6 Å. In oxy-Hc, the $\text{Cu}(II)$ ions are thought to be bridged by an oxygen molecule, in

- (1) Ibers, J. A.; Holm, R. H. *Science (Washington, D.C.)* **1980**, *209*, 223.
- (2) (a) Solomon, E. I.; Penfield, K. W.; Wilcox, D. E. *Struct. Bonding (Berlin)* **1983**, *53*, 1. (b) Solomon, E. I. *Metal Ions Biol.* **1981**, *3*, 41.
- (3) (a) Gaykema, W. P. J.; Volbeda, A.; Hol, W. G. J. *J. Mol. Biol.* **1985**, *187*, 255. (b) Linzen, B.; Soeter, N. M.; Riggs, A. F.; Schneider, H. J.; Schartau, W.; Moore, M. D.; Yokota, E.; Behrens, P. W.; Nakashima, H.; Takagi, T.; Nemoto, T.; Vereijken, J. M.; Bak, H. J.; Beintema, J. J.; Volbeda, A.; Gaykema, W. P. J.; Hol, W. G. J. *Science (Washington, D.C.)* **1985**, *229*, 519. (c) Gaykema, W. P. J.; Hol, W. G. J.; Vereijken, J. M.; Soeter, N. M.; Bak, H. J.; Beintema, J. J. *Nature (London)* **1984**, *309*, 23. (d) Volbeda, A.; Hol, W. G. J. *J. Mol. Biol.* **1989**, *531*.
- (4) (a) Spiro, T. G.; Wollery, G. L.; Brown, J. M.; Powers, L.; Winkler, M. E.; Solomon, E. I. In *Copper Coordination Chemistry; Biochemical and Inorganic Perspectives*; Karlin, K. D., Zubieta, J., Eds.; Adenine Press: Guilderland, NY, 1983; p 23. (b) Co, M. S.; Hodgson, K. O. *J. Am. Chem. Soc.* **1981**, *103*, 3200. (c) Co, M. S.; Hodgson, K. O.; Eccles, T. K.; Lontie, R. J. *Am. Chem. Soc.* **1981**, *103*, 984. (d) Brown, J. M.; Powers, L.; Kincaid, B.; Larrabee, J. A.; Spiro, T. G. *J. Am. Chem. Soc.* **1980**, *102*, 4210.

[†] University of Louisville.

[‡] University of Illinois.

[§] University of California at San Diego.

^{||} Centre d'Etudes Nucléaires de Grenoble.